JACS
JOURNAL OF THE AMERICAN CHEMICAL SOCIETY
pubs.acs.org/JACS
Article

Zn^{2+} Binds to Phosphatidylserine and Induces Membrane Blebbing

Matthew F. Poyton,[$] Saranya Pullanchery,[$] Simou Sun, Tinglu Yang, and Paul S. Cremer*

Cite This: J. Am. Chem. Soc. 2020, 142, 18679−18686
Read Online

ABSTRACT: Herein, we show that Zn^{2+} binds to phosphatidylserine (PS) lipids in supported lipid bilayers (SLBs), forming a PS-Zn^{2+} complex with an equilibrium dissociation constant of ∼100 μM. Significantly, Zn^{2+} binding to SLBs containing more than 10 mol % PS induces extensive reordering of the bilayer. This reordering is manifest through bright spots of high fluorescence intensity that can be observed when the bilayer contains a dye-labeled lipid. Measurements using atomic force microscopy (AFM) reveal that these spots represent three-dimensional unilamellar blebs. Bleb formation is ion specific, inducible by exposing the bilayer to μM concentrations of Zn^{2+} but not Mg^{2+}, Cu^{2+}, Co^{2+}, or Mn^{2+}. Moreover, Ca^{2+} can induce some blebbing at mM concentrations but not nearly as effectively as Zn^{2+}. The interactions of divalent metal cations with PS lipids were further investigated by a combination of vibrational sum frequency spectroscopy (VSFS) and surface pressure−area isotherm measurements. VSFS revealed that Zn^{2+} and Ca^{2+} were bound to the phosphate and carboxylate moieties on PS via contact ion pairing, dehydrating the lipid headgroup, whereas Mg^{2+} and Cu^{2+} were bound without perturbing the hydration of these functional groups. Additionally, Zn^{2+} was found to dramatically reduce the area per lipid in lipid monolayers, while Mg^{2+} and Cu^{2+} did not. Ca^{2+} could also reduce the area per lipid but only when significantly higher surface pressures were applied. These measurements suggest that Zn^{2+} caused lipid blebbing by decreasing the area per lipid on the side of the bilayer to which the salt was exposed. Such findings have implications for blebbing, fusion, oxidation, and related properties of PS-rich membranes in biological systems where Zn^{2+} concentrations are asymmetrically distributed.

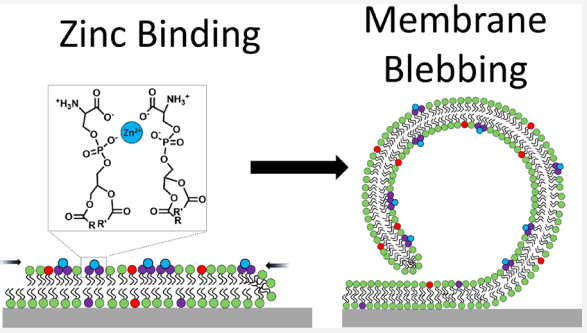

INTRODUCTION

The interactions of divalent metal cations with lipid bilayers influence numerous physiological processes. For example, Ca^{2+} binding to negatively charged lipids on the cytoplasmic leaflet of the cell membrane neutralizes the surface charge.[1] This leads to the release of positively charged membrane-bound proteins and activates cell-signaling cascades. The binding of divalent cations can also induce domain formation,[2−4] increase the gel to liquid crystalline phase transition temperature,[5] and promote vesicle aggregation and fusion.[6−10] Most studies probing the interactions of divalent cations with lipid bilayers have focused on Ca^{2+} and Mg^{2+} at mM concentrations. However, it has recently been shown that Cu^{2+} binds to phosphatidylserine (PS) headgroups with apparent picomolar affinity.[11,12] This discovery raises the question as to which other divalent metal cations bind to PS lipids with physiologically relevant affinities. Of particular interest is Zn^{2+}, the second most abundant d-block metal ion in the human body.[13] While the concentration of free intracellular Zn^{2+} has been measured to be in the picomolar range, local concentrations of labile Zn^{2+} can be quite high, reaching mM concentrations inside of secretory vesicles.[14]

Herein, we measured the affinity of Zn^{2+} for lipid membranes containing PS lipids using a competitive turn-on fluorescence assay. Fluorescence microscopy experiments utilizing dye-labeled supported lipid bilayers (SLBs) containing PS lipids revealed that aqueous solutions containing $ZnCl_2$ caused the appearance of micrometer-sized fluorescent spots on the membrane surface. Atomic force microscopy (AFM) experiments showed that these spots were actually three-dimensional unilamellar lipid blebs that budded off of the surface of the SLB upon exposure to Zn^{2+}. The formation of blebs on SLBs occurred with Zn^{2+} but not with Mg^{2+}, Cu^{2+}, Co^{2+}, or Mn^{2+}. The introduction of Ca^{2+} also led to some bleb formation, but the effect was significantly weaker than for Zn^{2+}. Moreover, vibrational sum frequency spectroscopy (VSFS) measurements showed that Zn^{2+} interacted with phosphate and carboxylate moieties on PS via contact ion pair formation (Figure 1A, top). Ca^{2+} also showed a propensity for ion pair formation. Mg^{2+} did not form contact ion pairs, and Cu^{2+} did not interact with the phosphate moiety.

Surface pressure−area isotherms demonstrated that Zn^{2+} condensed PS monolayers, suggesting that Zn^{2+} can dimerize

Received: August 24, 2020
Published: October 20, 2020

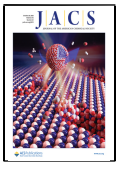

https://dx.doi.org/10.1021/jacs.0c09103
J. Am. Chem. Soc. 2020, 142, 18679−18686

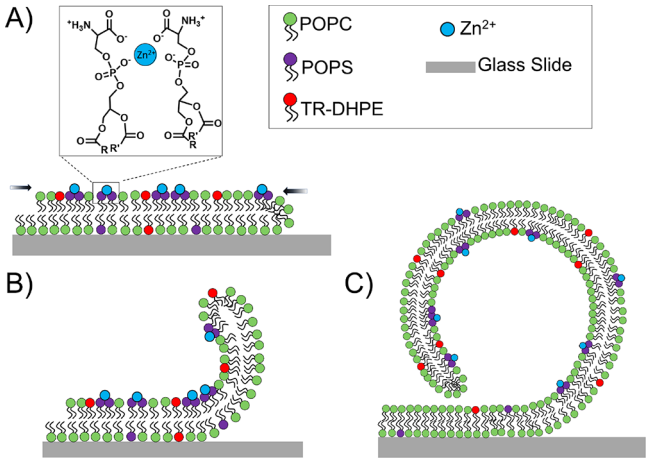

Figure 1. Proposed mechanism for bleb formation induced by Zn^{2+} binding to PS lipids in SLBs. (A) First, Zn^{2+} coordinates to two PS lipid headgroups and condenses the outer bilayer leaflet. This contraction is depicted by the two arrows in the image. (B) This initiates membrane bending, which (C) results in the formation of unilamellar blebs.

PS lipid. Ca^{2+} can do this too but only at significantly higher pressures that exceed the corresponding internal pressure found in bilayers (~30 mN/m).[15] The results for Zn^{2+} suggest that this ion can bind to the distal leaflet of supported bilayers, causing bleb formation by inducing curvature (Figure 1B). This asymmetry should arise because it is the distal leaflet that first comes into contact with the metal ions. The area mismatch between the distal and proximal leaflets results in the peeling of the lipid membranes off the surface (Figure 1B) and the subsequent formation of blebs (Figure 1C). This is reminiscent of the mechanism for blebbing induced by membrane proteins.[16,17] The current findings suggest that free Zn^{2+} should bind to PS-containing membranes in cells under conditions where Zn^{2+} is highly concentrated and that these binding events may significantly alter the physical properties of biomembranes.

RESULTS

Zn^{2+} Binds to Phosphatidylserine with High Micromolar Affinity. Zn^{2+} binding to lipid bilayers was monitored by a novel turn-on fluorescence assay that utilized SLBs made in microfluidic channels (Figure 2A). Figure 2B shows fluorescence line profiles across the red dashed lines in Figure 2A.

In this assay, SLBs were made with 20 mol % 1-palmitoyl-2-oleoyl-*sn*-glycero-3-phospho-L-serine (POPS), 79.5 mol % 1-palmitoyl-2-oleoyl-glycero-3-phosphocholine (POPC), and 0.5 mol % Texas Red-1,2-dihexadecanoyl-*sn*-glycero-3-phosphoethanolamine (TR-DHPE). In the left channel, Tris buffer was introduced without divalent metal cations (Figure 2A). In the middle channel, the SLBs were exposed to the same buffer but with 50 μM $NiCl_2$. In this case, the Ni^{2+} bound to the POPS lipids in the SLB and quenched the nearby TR-DHPE molecules. This result is analogous to previous experiments with Cu^{2+}.[11] Exposing the bilayer to 1 mM $ZnCl_2$ as well as 50 μM $NiCl_2$ unquenched the TR-DHPE (right channel). This turn-on in fluorescence signal was ion-specific, as exposing the same bilayers to buffer containing 50 μM $NiCl_2$ and 10 mM $CaCl_2$ did not lead to a full recovery of TR-DHPE fluorescence intensity (Figure S1). These experiments demonstrated that

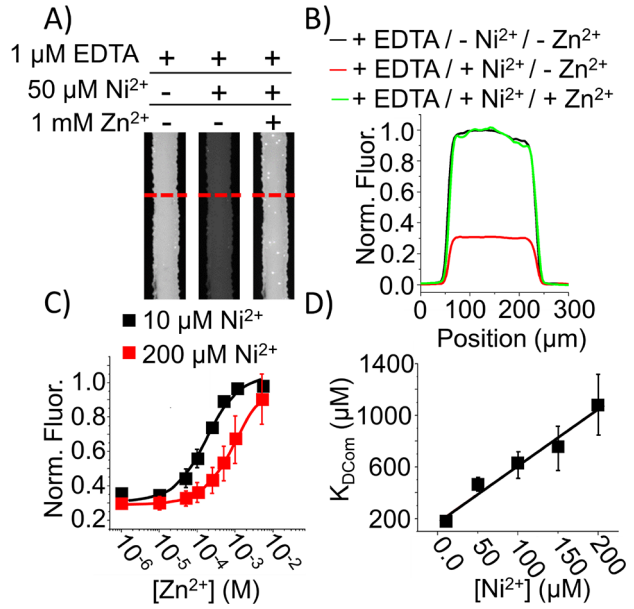

Figure 2. (A) SLB containing 20 mol % POPS and 0.5 mol % TR-DHPE in a microfluidic channel. The bilayer was exposed to buffer containing 1 μM EDTA in the leftmost channel, 1 μM EDTA and 50 μM $NiCl_2$ in the middle channel, and 1 μM EDTA, 50 μM $NiCl_2$, and 1 mM $ZnCl_2$ in the rightmost channel. Each channel was 200 μm in width. (B) The fluorescence intensity across the red dashed linescan in A is plotted for each solution condition. (C) Measurement of the fluorescence intensity from bilayers containing 20 mol % POPS and 0.5 mol % TR-DHPE exposed to a constant concentration of 10 μM $NiCl_2$ (black data points) and 200 μM $NiCl_2$ (red data points) and increasing concentrations of $ZnCl_2$. The solid lines are fits to the data and are described in more detail in the SI. (D) A plot of the measured apparent K_{DCom} values as a function of $NiCl_2$ concentration. The black line represents a linear fit to the data. All experiments were performed at 295 K.

sufficient concentrations of Zn^{2+} can out-compete Ni^{2+} for binding sites on PS lipid headgroups. It should be noted that the changes in the fluorescence only occurred in the presence of PS lipids. In fact, bilayers containing only PC and TR-DHPE showed no change in fluorescence intensity when exposed to $NiCl_2$ or $ZnCl_2$ (Figure S2).

Exposing the SLB to increasing concentrations of Zn^{2+} while holding the Ni^{2+} concentration constant caused the fluorescence of TR-DHPE to increase gradually before plateauing at the initial fluorescence intensity prior to being quenched by Ni^{2+} (Figure 2C). By fitting this fluorescence increase as a function of Zn^{2+} concentration to a Langmuir isotherm (see SI for details on curve fitting), it was possible to measure the apparent dissociation constant of the Zn^{2+}-PS lipid complex in an SLB containing 20 mol % POPS lipids in the presence of 10 μM Ni^{2+} (Figure 2C, black data points). The apparent dissociation constant measured in competition with Ni^{2+} is referred to as K_{DCom}. As expected, for competitive binding, K_{DCom} weakened from 190 ± 39 μM to 1.1 ± 0.25 mM as the concentration of Ni^{2+} was increased from 10 μM to 200 μM (Figure 2C, red data points). The intrinsic dissociation constant for the Zn^{2+}-PS complex in the absence of Ni^{2+} (K_{DInt}) could be extrapolated by measuring K_{DCom} values at various Ni^{2+} concentrations (Figure 2D, additional binding curves in Figure S3). The measured K_{DCom} value increased linearly with increasing Ni^{2+} concentration and should vary with Ni^{2+} concentration according to eq 1

https://dx.doi.org/10.1021/jacs.0c09103
J. Am. Chem. Soc. 2020, 142, 18679−18686

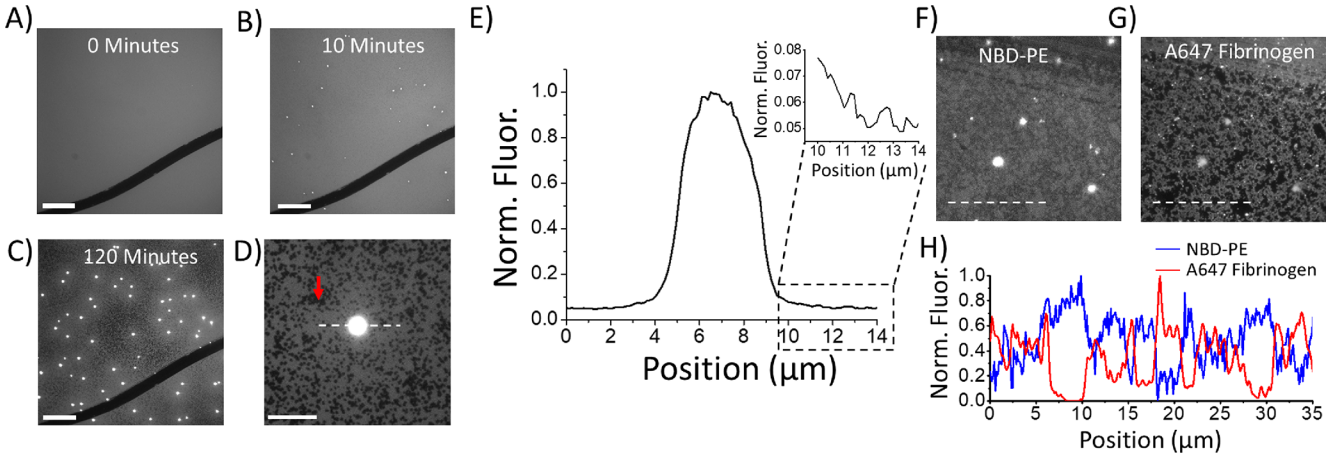

Figure 3. SLB composed of 30 mol % POPS/69.5 mol % POPC and 0.5 mol % TR-DHPE imaged at (A) 0 min, (B) 10 min, and (C) 120 min after the introduction of 100 μM Zn^{2+}. The scale bar in the images are 115 μm in length. (D) A spot from the same bilayer imaged under 100× magnification. The scale bar for this image is 12 μm in length, and the red arrow points to a region on the SLB with decreased fluorescence intensity. (E) A fluorescence intensity line scan across the dashed white line in (D). The inset is a zoom in of the fluorescence intensity directly adjacent to the bright spot. (F) NBD-PE fluorescence micrograph from an SLB composed of 30 mol % POPS/69.5 mol % POPC and 0.5 mol % NBD-PE exposed first to 100 μM Zn^{2+} and then to A647 fibrinogen. (G) An image of A647 fibrinogen after washing the same bilayer with buffer. The length of the dashed white lines in both F and G is 35 μm. (H) The fluorescence intensity of both NBD-PE and A647 fibrinogen over the dashed white lines in F and G. All experiments were performed at 295 K.

$$K_{DCom} = K_{DInt} \times \left(1 + \frac{[Ni^{2+}]}{K_D^{Ni^{2+}}}\right) \quad (1)$$

In eq 1, $[Ni^{2+}]$ is the concentration of Ni^{2+} in bulk solution and $K_D^{Ni^{2+}}$ is the dissociation constant for the Ni^{2+}-PS complex. Fitting eq 1 to the data points in Figure 2D yields a K_{DInt} value of 100 μM ± 33 μM, a reasonable dissociation constant based on measured affinities of other divalent cations for PS lipids[12] and the Irving-Williams series.[18] The $K_D^{Ni^{2+}}$ value of 37 ± 15 μM obtained from the linear fit is also reasonable when taking into account surface charge effects (Figures S4 and S5 as well as the associated discussion).

Zn^{2+} Binding to PS Lipids Causes Membrane Blebbing. Curiously, micrometer-sized bright spots were observed on the surface of the SLB upon exposure to Zn^{2+} in the binding curve measurements. To explore this further, SLBs were formed with 30 mol % POPS/69.5 mol % POPC and 0.5 mol % TR-DHPE on glass coverslips and exposed to 100 μM Zn^{2+}. It should be noted that the increase in POPS concentration from 20 mol % to 30 mol % was made in order to maximize the observed number of bright spots.

The bilayer was initially uniform in its appearance (Figure 3A), but bright spots began to appear several minutes after being exposed to Zn^{2+} (Figure 3B). The number density and size of the spots increased over time before reaching a steady state after about 2 h (Figure 3C). In the absence of Zn^{2+}, the bilayers did not change in appearance over the same 2-h timespan (Figure S6). Imaging the SLBs at higher magnification revealed that regions of decreased fluorescence intensity also appeared on the bilayer surface (Figure 3D, red arrow). Moreover, a line scan across the micrograph at high magnification (Figure 3E, across the white-dashed line in Figure 3D) showed that the fluorescence intensity of a typical bright spot was between one and 2 orders of magnitude higher than the surrounding bilayer. This ratio was determined by comparing the maximum intensity from the bright spot in Figure 3E with the bilayer intensity next to it (the inset in Figure 3E shows the fluorescence level from the adjacent bilayer). These results suggested that material was transferred from the surrounding SLB to the smaller regions of bright intensity upon Zn^{2+} exposure.

To test whether the regions of low fluorescence intensity were holes in the bilayer or domains where the fluorescent dye was merely depleted, nascently formed SLBs were first exposed to 100 μM Zn^{2+} and then to 0.001 mg/mL fibrinogen labeled with Alexa-647 (A647 fibrinogen, Figure 3F,G). In this case, the SLB was labeled with NBD-PE to avoid fluorescence resonant energy transfer (FRET) with A647 fibrinogen.[19] Dye-labeled fibrinogen is known to stick to bare glass but not to lipid bilayers.[20] Imaging, after excess fibrinogen was washed away, revealed that the protein was adsorbed to the dark spots but not to the bilayer surface (Figure 3F,G). A line scan across the micrograph revealed that the intensity from A647-fibrinogen and NBD-PE were anticorrelated (Figure 3H), indicating that the dark regions were in fact holes in the SLB.

The formation of bright spots upon exposure to Zn^{2+} was limited to bilayers containing PS lipids. In fact, bilayers containing other negatively charged lipids, like 1-palmitoyl-2-oleoyl-*sn*-glycero-3-phospho-(1′-rac-glycerol) (POPG), did not form bright spots under similar conditions (Figure S7A). Also, the exact nature of the alkyl chain tails was not particularly important for spot formation (Figure S7B). Bright spots, however, did not form if the lipids were in the gel phase (Figure S7C). Most importantly, the formation of bright spots was found to be cation specific. Exposing the bilayers to Mg^{2+}, Cu^{2+}, Ni^{2+}, Co^{2+}, and Mn^{2+} did not cause the fluorescence intensity to become nonuniform (Figure S8). However, exposing SLBs containing 30 mol % POPS in POPC to 10 mM Ca^{2+} did produce some bright spots on the bilayer surface. These spots were not as circular or intense as the bright spots produced upon the addition of Zn^{2+} (Figure S9).

Bright Spots Show Fluorescence Recovery. Fluorescence recovery after photobleaching (FRAP)[21] experiments revealed that the bright spots represented regions on the membrane surface that were two-dimensionally fluid and

https://dx.doi.org/10.1021/jacs.0c09103
J. Am. Chem. Soc. 2020, 142, 18679−18686

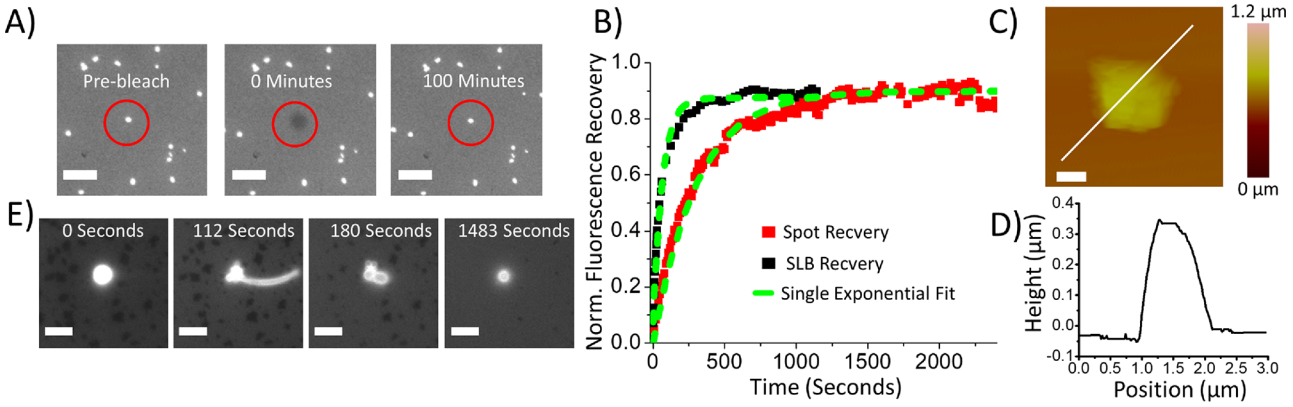

Figure 4. SLB composed of 30 mol % POPS/69.5 mol % POPC and 0.5 mol % TR-DHPE was exposed to 100 μM Zn^{2+} for 2 h. The first image in (A) shows the bilayer immediately before bleaching, the middle image is immediately after bleaching and the last image is 100 min after bleaching. The bleached spot is denoted by a red circle. The scale bar in each image is 24 μm in length. (B) Normalized fluorescence recovery plotted as a function of time for the bright spot (red squares) as well as for a bilayer region not containing any spots (black squares). The dashed green lines are single exponential fits to the recovery for these two regions. (C) A tapping mode AFM micrograph of a 3D bleb from the bilayer after exposure to 1 mM Zn^{2+}. The white scale bar in the image is 750 nm in length. (D) The height profile for the feature over the white line scan in (C). (E) Images of a spot immediately prior to exposure to Tris buffer containing 100 μM EDTA and at 112 s, 180 and 1483 s after introducing 100 μM EDTA. The scale bar in the image is 8 μm in length. All experiments were performed at 295 K.

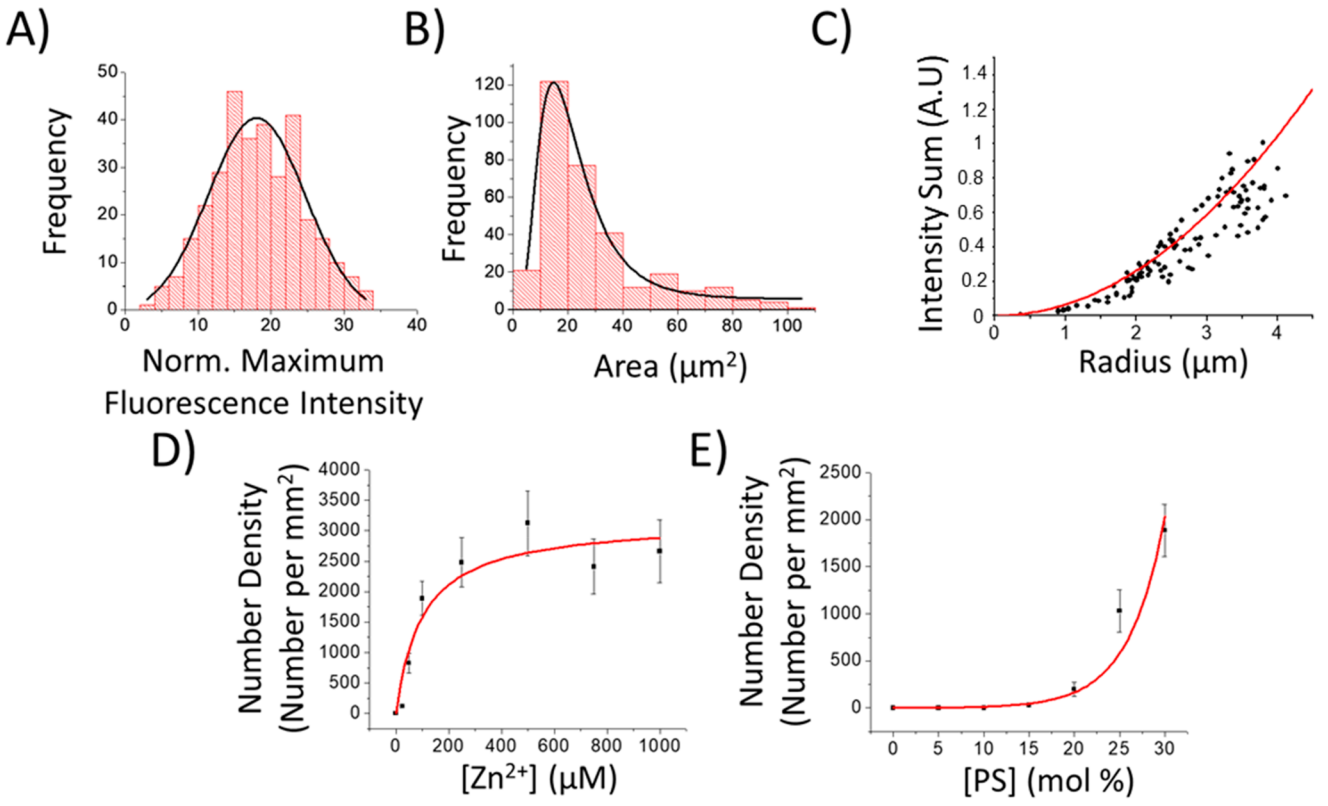

Figure 5. (A) Histogram of the maximum fluorescence intensity normalized to the intensity of the surrounding SLB for 324 blebs from three separate SLBs. The black line is a Gaussian peak fit to the data. (B) A histogram of the spot area taken from the same 324 blebs in (A). The black line is a log-normal fit to the data points. (C) Plot of the Intensity Sum for all pixels in the images of 128 individual blebs as a function of bleb radius. The red line represents the value of the expected bleb intensity as a function of the radius determined from a model for unilamellar bleb formation (see Intensity Model for a Unilamellar Bleb Formed on a Supported Lipid Bilayer in the SI). (D) The number density of spots formed on an SLB containing 30 mol % POPS exposed to buffer containing different concentrations of Zn^{2+}. The red line is a Langmuir isotherm fit to the data. (E) The number density of spots formed on SLBs containing increasing concentrations of POPS lipids exposed to 100 μM Zn^{2+}. The red line is an exponential fit to the data. All experiments were performed at 295 K.

connected to the rest of the SLB. After being photobleached, the fluorescence of the bright spots recovered over time (Figure 4A). The speed of fluorescence recovery, however, was significantly slower for these spots than for regions of the SLB adjacent to them (Figure 4B). The recovery curve from the bright spots fit well to a single exponential function, from which the mobile fraction and diffusion coefficient of the TR-DHPE fluorophores in the bright spot could be obtained (see

https://dx.doi.org/10.1021/jacs.0c09103
J. Am. Chem. Soc. 2020, 142, 18679−18686

SI for details of the FRAP analysis). The diffusion coefficient and mobile fraction from the bright spots were 0.027 ± 0.003 $\mu m^2/s$ and 93 ± 6%, respectively, whereas the diffusion coefficient and mobile fraction from the surrounding bilayer were 0.83 ± 0.06 $\mu m^2/s$ and 93 ± 3%. As such, the apparent diffusion coefficient in the region of the bright spot was 31 ± 4 times slower than diffusion throughout the rest of the SLB, although the mobile fractions were similar.

The slow diffusion coefficient suggested that the bright spots were either two-dimensional liquid-crystalline domains or three-dimensional blebs budding off the surface. This ambiguity was resolved using underwater tapping mode atomic force microscopy (AFM; see SI for details), which clearly showed the presence of protrusions from the bilayer surface that were hundreds of nm tall (Figure 4C,D). These features were not observed in bilayers that were not exposed to Zn^{2+}. Due to their three-dimensional nature, these features could be described as lipid blebs. Bleb formation could be partially reversed by exposing the bilayers to 100 μM EDTA (Figure 4E). As can be seen, unusually shaped blebs and vesicle features were observed during the dissolution process. Specifically, the image at 112 s shows a tubule budding off from the bright spot, while several round structures appear to form at 180 s.

Constructing Histograms. The fluorescence intensity from the blebs was many times greater than those of the surrounding bilayers. A histogram of the maximum fluorescence intensity of each bright spot revealed a Gaussian distribution with a mean that was 18 times as bright as the surrounding SLB (Figure 5A). A histogram of the two-dimensional area of a bleb fit to a log-normal distribution (Figure 5B; see SI for fitting details). The mean area of the blebs was 29 ± 1 μm^2. Assuming the fluorophore density per unit area was equal for both the blebs and the adjacent SLB, the total fluorescence intensity over all pixels from a bleb (Intensity Sum, Figure 5C), plotted as a function of bleb radius, matches the predicted intensity for unilamellar vesicles of varying radius (red line in Figure 5C). Details for the model of unilamellar bleb intensity are provided in the SI.

The density of the blebs formed on the SLB was dependent upon the concentration of Zn^{2+} in the buffer above the supported bilayer. For bilayers containing 30 mol % POPS, blebs appeared on the bilayer surface at Zn^{2+} concentrations as low as 25 μM (120 ± 21 dots/mm^2) (Figure 5D). The density of spots increased with Zn^{2+} concentration up to 2660 ± 520 spots/mm^2 for SLBs exposed to 1 mM Zn^{2+}. As can be seen, the spot density increased as a function of Zn^{2+} concentration similarly to a binding curve and could be well-fit to a Langmuir isotherm (red curve in Figure 5D) with an equilibrium dissociation constant of 87 μM, which is quite close to the 100 μM K_{DInt} value determined by the Ni^{2+}-Zn^{2+} competition assay (Figure 2). The bleb density was also dependent on the concentration of PS lipids in the membrane. Figure 5E plots the number of blebs formed per mm^2 of bilayer upon exposure to 100 μM Zn^{2+}. No blebs were formed when the PS concentration was less than 10 mol %. However, the density of spots increased exponentially above this concentration (the red line is an exponential fit to the data).

Mechanism of Ion Specificity for Bleb Formation. In a last set of experiments, vibrational sum frequency spectroscopy (VSFS) and surface pressure−area isotherms were employed to study the molecular level interactions involved in Zn^{2+} binding to PS. Langmuir monolayers of 1,2-dilauroyl-*sn*-glycero-3- phosphoserine (DLPS) were exposed to $ZnCl_2$, $CaCl_2$, $MgCl_2$, and $CuCl_2$, respectively, in the subphase. DLPS was used in these experiments instead of POPS to avoid oxidation of the alkyl chains.[22] The salt concentrations were chosen to be above the K_D values for the respective ions. The phosphate symmetric stretch frequency around 1105 cm^{-1} was found to change in an ion-specific manner (Figure 6A). In fact,

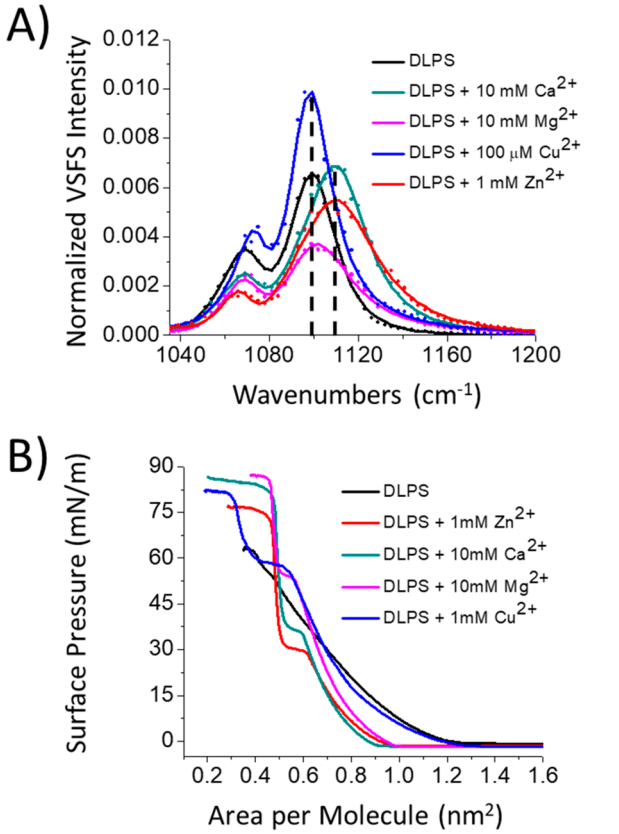

Figure 6. (A) VSFS spectra of the phosphate stretch from DLPS monolayers in the absence (black) and presence of different divalent metal cation chloride salts. The dashed black vertical lines highlight the blue shift that is seen upon the addition of $CaCl_2$ and $ZnCl_2$. The surface pressure was fixed at 30 mN/m in all cases. (B) Surface pressure−area isotherms of DLPS monolayers in the absence and presence of the same divalent metal cation chloride salts. All experiments were performed at 295 K. See the SI section for details on the salt concentrations that were employed in these experiments as well as for additional information the interpretation of the VSFS spectra.

changes in the intensity, peak width, and center frequency could be observed depending on the nature of the cation. Modulation of the intensity and peak width was largely governed by a combination of changes in orientation and ordering of the phosphate moiety within the monolayer as the various salts were introduced.[23,24] More significantly, the center frequency exhibited a blue-shift when the cations formed contact pairs with the phosphate group.[24−28] The frequency remained unchanged, however, for cations that formed solvent shared ion pairs with the phosphate group or did not interact with it at all.

As can be seen in Figure 6A, the addition of 1 mM Zn^{2+} or 10 mM Ca^{2+} to the subphase blue-shifted the phosphate symmetric stretch by 13 and 7 cm^{-1}, respectively, with respect to conditions without added salt (Figure 6A, red (Zn^{2+}) and

https://dx.doi.org/10.1021/jacs.0c09103
J. Am. Chem. Soc. 2020, 142, 18679−18686

dark green (Ca^{2+}) spectra vs the black spectrum). In contrast, Mg^{2+} ions did not shift the phosphate symmetric stretch frequency (pink spectrum in Figure 6A). The lack of a spectral shift in this case is consistent with Mg^{2+} binding to the phosphate moieties via a solvent shared ion pairing interaction.[29] The phosphate symmetric stretch spectrum in the presence of 100 μM Cu^{2+} ions (blue spectrum in Figure 6A) agrees with existing information on the formation of a square planar complex between Cu^{2+} and two carboxylate and two amine moieties on adjacent lipid headgroups.[11,12,30] Namely, there was no shift in the phosphate symmetric stretch frequency, as Cu^{2+} did not bind to the phosphate moiety. All the ions tested here were found to interact with the carboxylate moieties on the headgroup (Figure S10). Analysis of the carboxylate stretch, however, is more convoluted because of overlap between the COO^- and C−H modes in this spectral window.[31]

Since the VSFS spectra indicated that Zn^{2+} and Ca^{2+} formed contact ion pairs with the phosphate moieties, the question arises as to whether these ions can also alter the average area per lipid headgroup, as this would help induce membrane curvature and blebbing.[32,33] To address this question, surface pressure−area isotherm measurements with DLPS monolayers were made in the presence and absence of all four divalent cation salts (Figure 6B). DLPS monolayers in the absence of divalent cations gave rise to a simple liquid expanded phase throughout the course of compression (black curve).[34] As can be seen, the addition of Zn^{2+} and Ca^{2+} caused the biggest decrease in lipid headgroup area, followed by Mg^{2+}. By contrast, the area per lipid headgroup in the presence of Cu^{2+} did not change significantly, which is consistent with Cu^{2+} binding to PS lipid headgroups without neutralizing their negative charge.[12] As such, the Cu^{2+}-PS lipid complexes remained electrostatically repulsive. This was not the case for Ca^{2+}, Mg^{2+}, and Zn^{2+}, which neutralized the charge on the PS lipid headgroups, making the monolayers easier to compress.

The isotherms revealed that all ions induced a phase transition from the liquid-expanded phase to the liquid-condensed phase (plateau regions in Figure 6B just below 0.6 nm^2).[35] Critically, the plateau occurred near 30 mN/m with Zn^{2+} but around 37 mN/m with Ca^{2+}. As such, Zn^{2+} is more effective than Ca^{2+} at decreasing the area per lipid. This may explain why Zn^{2+} is also more effective at bleb formation compared with Ca^{2+}. At the molecular level, this may be a result of a difference in the ratio of ion binding to phosphate versus carboxylate moieties, but a slight affinity of Zn^{2+} for the amine group may also contribute, which is not the case for Ca^{2+}.[28,36] Finally, Mg^{2+} and Cu^{2+} were only able to induce the liquid-expanded to liquid-condensed phase transition at very high two-dimensional pressures (above 45 mN/m). This is consistent with the need for contact ion pair formation with phosphate groups in order to induce lipid area contraction at lower two-dimensional pressures.

DISCUSSION

Physical Chemistry of Zn^{2+}-Induced Lipid Blebbing from Supported Bilayers. The data provided above demonstrate that Zn^{2+} binds to PS lipid headgroups, forming a complex with a dissociation constant of ∼100 μM. Consistent with the Irving-Williams series, first row transition metal ion binding affinities follow the order: Zn^{2+}< Ni^{2+}< Cu^{2+}.[11,18] Nevertheless, among these three ions, only Zn^{2+} induces extensive membrane blebbing. To a lesser extent, Ca^{2+} can also induce blebbing, but Mn^{2+}, Co^{2+}, and Mg^{2+} do not. The finding for Ca^{2+} is consistent with recent work demonstrating that this ion induces membrane bending in giant unilamellar vesicles (GUVs) containing PS lipids much more effectively than Mg^{2+}.[33] As proposed herein, it should be contact ion pairing with the phosphate moiety and the concomitant contraction of the area per lipid that leads to blebbing (Figure 1).

The glass coverslips, upon which supported bilayers sit, are negatively charged.[37] As such, more than half of the PS lipid should reside in the outer bilayer leaflet of a supported bilayer on electrostatic grounds.[38] Moreover, divalent cations will encounter the outer leaflet first. When Zn^{2+} binds to PS lipids, the area per lipid in the outer leaflet will shrink, while the area per lipid on the inner leaflet will remain essentially unchanged (Figure 1A). Membrane bending occurs in order to accommodate this asymmetric area change (Figure 1B). This is what ultimately causes the bilayer to start peeling away from the glass surface. Such changes eventually lead to the rolling up of the membrane into unilamellar blebs (Figure 1C). Since supported bilayers contain edge defect sites,[39] these are the logical starting points from which blebs should nucleate.

While two-dimensional phase separated domains form readily on supported bilayers, the formation of stable three-dimensional lipid blebs is surprising as the adhesion energy of bilayers to the glass surface is significant.[40] The driving force to form membrane blebs is evidentially quite substantial, as seen by the appearance and growth of holes in the SLB as blebs form and grow (Figure 3D). As a check to test whether the free energy change which occurs when Zn^{2+} binds to PS lipids is sufficient to cause blebbing, the energy required to delaminate a bilayer from the glass surface was calculated. This calculation used the average surface area of a bleb (29 μm^2) and also took into account the energy required to bend a patch of bilayer into a lipid vesicle (see SI for details). The calculated energetic cost of bleb formation, 23 fJ, is 40 times less than the binding energy of Zn^{2+} to an SLB containing 30 mol % PS lipids (−900 fJ), which was calculated by using the measured dissociation constant of 100 μM at 295 K. As such, the bleb formation process is expected to be thermodynamically favorable.

Biological Relevance of Zn^{2+} Binding to PS Lipid Headgroups. Like the SLBs used in these experiments, cell membranes are asymmetric, with essentially all the PS lipids found in the cytoplasmic leaflet.[41] The concentration of labile intracellular Zn^{2+} is tightly regulated and is normally in the picomolar concentration range.[42] Therefore, Zn^{2+} should not be bound to PS lipids on the plasma membrane under most instances. Indeed, one reason to regulate the concentration of intracellular Zn^{2+} may be to prevent it from interacting with cellular membranes and adjusting their physical properties. It is known that Zn^{2+} prevents Fe^{2+} mediated lipid oxidation via a mechanism that is still not well understood.[43] Our results suggest that this antioxidant effect could be due to the ability of Zn^{2+} to compete for binding sites on the lipid membrane with metal ions that produce reactive oxygen species (e.g., Cu^{2+} or Fe^{2+}) under circumstances where the concentration of both types of ions is elevated.

While tightly regulated, there are specific locations where labile intracellular Zn^{2+} is found at high concentration.[14,42] One of the best characterized areas where labile Zn^{2+} can be found is in axon terminals of neurons in the forebrain. This pool of intracellular labile zinc ions is contained in synaptic vesicles, reaching mM concentrations.[42,44] Specifically, labile

https://dx.doi.org/10.1021/jacs.0c09103
J. Am. Chem. Soc. 2020, 142, 18679−18686

Zn^{2+} is stored in vesicles in mammalian oocytes. The concentration of Zn^{2+} in these vesicles has been reported to be 200 mM.[14] While the lipid composition of vesicles found in oocytes is not known, the lipid membranes of synaptic vesicles contain 12% PS lipids.[45] As such, Zn^{2+} should be bound to PS lipids in such vesicles and may help induce membrane blebbing.

The contents of both synaptic vesicles and zinc-containing vesicles in oocytes are released outside the cell via exocytosis. Zn^{2+} bound to the lipid membranes of these vesicles may change the physical properties of the bilayer and thereby modulate fusion with the cytoplasmic lipid membrane. Finally, Zn^{2+} induced changes to the physical properties of the lipid membrane are also likely to alter the function of membrane proteins, either by preventing positively charged proteins from binding to the membrane surface or by changing the phase of the lipid membrane. Indeed, cells might utilize Zn^{2+} fluxes to convey information in significant ways by altering the physical properties of lipid membranes.

CONCLUSION

This work demonstrates that Zn^{2+} can bind to phosphatidylserine lipid headgroups forming a complex with a dissociation constant of approximately 100 μM. Such binding can induce membrane blebbing. Chemically specific criteria were also determined by which bivalent metal cations can induce lipid blebbing. First, an ion should bind via contact ion pairing to the phosphate moiety on the headgroup and neutralize the charge on the bilayer. Second, the ion must change the average area per lipid headgroup in order to bend the bilayer. These rules point to Zn^{2+} having a special ability to induce blebbing, although Ca^{2+} can do this to a lesser extent. Going forward, the ability of Zn^{2+} to act as a secondary messenger by changing the physical properties of lipid membranes *in vivo* should be explored.

ASSOCIATED CONTENT

Supporting Information

The Supporting Information is available free of charge at https://pubs.acs.org/doi/10.1021/jacs.0c09103.

Materials and methods for cleaning glass coverslips, forming microfluidic devices, preparing lipid vesicles and supported lipid bilayers, imaging and FRAP measurements of supported lipid bilayers, conditions for the Ni^{2+}-Zn^{2+} competitive assay, fibrinogen staining, vibrational sum frequency spectroscopy, surface-pressure area isotherms, atomic force microscopy, fitting binding curves, the unilamellar bleb intensity model, the calculation of the interaction energy for the SLB and glass substrate, fitting parameters for the VSFS spectra as well as supporting figures (PDF)

AUTHOR INFORMATION

Corresponding Author

Paul S. Cremer − *Department of Chemistry and Department of Biochemistry and Molecular Cell Biology, The Pennsylvania State University, University Park, Pennsylvania 16802, United States;* orcid.org/0000-0002-8524-0438; Email: psc11@psu.edu

Authors

Matthew F. Poyton − *Department of Chemistry, The Pennsylvania State University, University Park, Pennsylvania 16802, United States;* orcid.org/0000-0003-1261-2138

Saranya Pullanchery − *Department of Chemistry, The Pennsylvania State University, University Park, Pennsylvania 16802, United States;* orcid.org/0000-0002-7011-0788

Simou Sun − *Department of Chemistry, The Pennsylvania State University, University Park, Pennsylvania 16802, United States;* orcid.org/0000-0002-0596-1156

Tinglu Yang − *Department of Chemistry, The Pennsylvania State University, University Park, Pennsylvania 16802, United States;* orcid.org/0000-0003-0872-8218

Complete contact information is available at: https://pubs.acs.org/10.1021/jacs.0c09103

Author Contributions

$M.F.P. and S.P. contributed equally.

Notes

The authors declare no competing financial interest.

ACKNOWLEDGMENTS

We acknowledge the National Science Foundation (CHE1709735) for funding this project.

REFERENCES

(1) Shi, X.; Bi, Y.; Yang, W.; Guo, X.; Jiang, Y.; Wan, C.; Li, L.; Bai, Y.; Guo, J.; Wang, Y.; Chen, X.; Wu, B.; Sun, H.; Liu, W.; Wang, J.; Xu, C. Ca^{2+} regulates T-cell receptor activation by modulating the charge property of lipids. *Nature* **2013**, *493*, 111.

(2) Ross, M.; Steinem, C.; Galla, H.-J.; Janshoff, A. Visualization of Chemical and Physical Properties of Calcium-Induced Domains in DPPC/DPPS Langmuir-Blodgett Layers. *Langmuir* **2001**, *17* (8), 2437−2445.

(3) Schultz, Z. D.; Pazos, I. M.; McNeil-Watson, F. K.; Lewis, E. N.; Levin, I. W. Magnesium-Induced Lipid Bilayer Microdomain Reorganizations: Implications for Membrane Fusion. *J. Phys. Chem. B* **2009**, *113* (29), 9932−9941.

(4) Kensbock, R.; Ahrens, H.; Helm, C. A. Interactions of Monovalent and Divalent Cations with Cardiolipin Monolayers. *Langmuir* **2019**, *35* (10), 3624−3633.

(5) Silvius, J. R.; Gagne, J. Lipid phase behavior and calcium-induced fusion of phosphatidylethanolamine-phosphatidylserine vesicles. Calorimetric and fusion studies. *Biochemistry* **1984**, *23* (14), 3232−3240.

(6) Düzgünes, N.; Nir, S.; Wilschut, J.; Bentz, J.; Newton, C.; Portis, A.; Papahadjopoulos, D. Calcium- and magnesium-induced fusion of mixed phosphatidylserine/phosphatidylcholine vesicles: Effect of ion binding. *J. Membr. Biol.* **1981**, *59* (2), 115−125.

(7) Wilschut, J.; Hoekstra, D. Membrane fusion: from liposomes to biological membranes. *Trends Biochem. Sci.* **1984**, *9* (11), 479−483.

(8) Papahadjopoulos, D.; Nir, S.; Düzgünes, N. Molecular mechanisms of calcium-induced membrane fusion. *J. Bioenerg. Biomembr.* **1990**, *22* (2), 157−179.

(9) Liu, Y.; Liu, J. Cu^{2+}-Directed Liposome Membrane Fusion, Positive-Stain Electron Microscopy, and Oxidation. *Langmuir* **2018**, *34* (25), 7545−7553.

(10) Liu, Y.; Liu, J. Zn^{2+} Induced Irreversible Aggregation, Stacking, and Leakage of Choline Phosphate Liposomes. *Langmuir* **2017**, *33* (50), 14472−14479.

(11) Monson, C. F.; Cong, X.; Robison, A. D.; Pace, H. P.; Liu, C.; Poyton, M. F.; Cremer, P. S. Phosphatidylserine Reversibly Binds Cu^{2+} with Extremely High Affinity. *J. Am. Chem. Soc.* **2012**, *134* (18), 7773−7779.

(12) Cong, X.; Poyton, M. F.; Baxter, A. J.; Pullanchery, S.; Cremer, P. S. Unquenchable Surface Potential Dramatically Enhances Cu^{2+}

Binding to Phosphatidylserine Lipids. *J. Am. Chem. Soc.* **2015**, *137* (24), 7785−7792.
(13) Lim, N. C.; Freake, H. C.; Brückner, C. Illuminating Zinc in Biological Systems. *Chem. - Eur. J.* **2005**, *11* (1), 38−49.
(14) Que, E. L.; Bleher, R.; Duncan, F. E.; Kong, B. Y.; Gleber, S. C.; Vogt, S.; Chen, S.; Garwin, S. A.; Bayer, A. R.; Dravid, V. P.; Woodruff, T. K.; O'Halloran, T. V. Quantitative mapping of zinc fluxes in the mammalian egg reveals the origin of fertilization-induced zinc sparks. *Nat. Chem.* **2015**, *7*, 130.
(15) Marsh, D. Lateral pressure in membranes. *Biochim. Biophys. Acta, Rev. Biomembr.* **1996**, *1286* (3), 183−223.
(16) Zimmerberg, J.; Kozlov, M. M. How proteins produce cellular membrane curvature. *Nat. Rev. Mol. Cell Biol.* **2006**, *7*, 9.
(17) Stachowiak, J. C.; Brodsky, F. M.; Miller, E. A. A cost−benefit analysis of the physical mechanisms of membrane curvature. *Nat. Cell Biol.* **2013**, *15* (9), 1019−1027.
(18) Irving, H.; Williams, R. J. P. 637. The stability of transition-metal complexes. *J. Chem. Soc.* **1953**, No. 0, 3192−3210.
(19) Loura, L.; Prieto, M. FRET in Membrane Biophysics: An Overview. *Front. Physiol.* **2011**, *2*, 82.
(20) Glasmästar, K.; Larsson, C.; Höök, F.; Kasemo, B. Protein Adsorption on Supported Phospholipid Bilayers. *J. Colloid Interface Sci.* **2002**, *246* (1), 40−47.
(21) Axelrod, D.; Koppel, D. E.; Schlessinger, J.; Elson, E.; Webb, W. W. Mobility measurement by analysis of fluorescence photobleaching recovery kinetics. *Biophys. J.* **1976**, *16* (9), 1055−1069.
(22) Liljeblad, J. F. D.; Bulone, V.; Tyrode, E.; Rutland, M. W.; Johnson, C. M. Phospholipid Monolayers Probed by Vibrational Sum Frequency Spectroscopy: Instability of Unsaturated Phospholipids. *Biophys. J.* **2010**, *98* (10), L50−L52.
(23) Pullanchery, S.; Yang, T.; Cremer, P. S. Introduction of Positive Charges into Zwitterionic Phospholipid Monolayers Disrupts Water Structure Whereas Negative Charges Enhances It. *J. Phys. Chem. B* **2018**, *122* (51), 12260−12270.
(24) Casillas-Ituarte, N. N.; Chen, X.; Castada, H.; Allen, H. C. Na^+ and Ca^{2+} Effect on the Hydration and Orientation of the Phosphate Group of DPPC at Air-Water and Air-Hydrated Silica Interfaces. *J. Phys. Chem. B* **2010**, *114* (29), 9485−9495.
(25) Casal, H. L.; Mantsch, H. H.; Hauser, H. Infrared studies of fully hydrated saturated phosphatidylserine bilayers. Effect of lithium and calcium. *Biochemistry* **1987**, *26* (14), 4408−4416.
(26) Casal, H. L.; Mantsch, H. H.; Paltauf, F.; Hauser, H. Infrared and 31P-NMR studies of the effect of Li^+ and Ca^{2+} on phosphatidylserines. *Biochim. Biophys. Acta, Lipids Lipid Metab.* **1987**, *919* (3), 275−286.
(27) Dluhy, R.; Cameron, D. G.; Mantsch, H. H.; Mendelsohn, R. Fourier transform infrared spectroscopic studies of the effect of calcium ions on phosphatidylserine. *Biochemistry* **1983**, *22* (26), 6318−6325.
(28) Melcrová, A.; Pokorna, S.; Pullanchery, S.; Kohagen, M.; Jurkiewicz, P.; Hof, M.; Jungwirth, P.; Cremer, P. S.; Cwiklik, L. The complex nature of calcium cation interactions with phospholipid bilayers. *Sci. Rep.* **2016**, *6*, 38035.
(29) Bilkova, E.; Pleskot, R.; Rissanen, S.; Sun, S.; Czogalla, A.; Cwiklik, L.; Róg, T.; Vattulainen, I.; Cremer, P. S.; Jungwirth, P.; Coskun, Ü. Calcium Directly Regulates Phosphatidylinositol 4,5-Bisphosphate Headgroup Conformation and Recognition. *J. Am. Chem. Soc.* **2017**, *139* (11), 4019−4024.
(30) Kusler, K.; Odoh, S. O.; Silakov, A.; Poyton, M. F.; Pullanchery, S.; Cremer, P. S.; Gagliardi, L. What Is the Preferred Conformation of Phosphatidylserine−Copper(II) Complexes? A Combined Theoretical and Experimental Investigation. *J. Phys. Chem. B* **2016**, *120* (50), 12883−12889.
(31) Liljeblad, J. F. D.; Bulone, V.; Rutland, M. W.; Johnson, C. M. Supported Phospholipid Monolayers. The Molecular Structure Investigated by Vibrational Sum Frequency Spectroscopy. *J. Phys. Chem. C* **2011**, *115* (21), 10617−10629.
(32) McMahon, H. T.; Gallop, J. L. Membrane curvature and mechanisms of dynamic cell membrane remodelling. *Nature* **2005**, *438*, 590.
(33) Graber, Z. T.; Shi, Z.; Baumgart, T. Cations induce shape remodeling of negatively charged phospholipid membranes. *Phys. Chem. Chem. Phys.* **2017**, *19* (23), 15285−15295.
(34) Mattai, J.; Hauser, H.; Demel, R. A.; Shipley, G. G. Interactions of metal ions with phosphatidylserine bilayer membranes: effect of hydrocarbon chain unsaturation. *Biochemistry* **1989**, *28* (5), 2322−2330.
(35) Kewalramani, S.; Hlaing, H.; Ocko, B. M.; Kuzmenko, I.; Fukuto, M. Effects of Divalent Cations on Phase Behavior and Structure of a Zwitterionic Phospholipid (DMPC) Monolayer at the Air-Water Interface. *J. Phys. Chem. Lett.* **2010**, *1* (2), 489−495.
(36) Takagishi, T.; Okuda, S.; Kuroki, N.; Kozuka, H. Binding of metal ions by polyethylenimine and its derivatives. *J. Polym. Sci., Polym. Chem. Ed.* **1985**, *23* (8), 2109−2116.
(37) Cremer, P. S.; Boxer, S. G. Formation and Spreading of Lipid Bilayers on Planar Glass Supports. *J. Phys. Chem. B* **1999**, *103* (13), 2554−2559.
(38) Shreve, A. P.; Howland, M. C.; Sapuri-Butti, A. R.; Allen, T. W.; Parikh, A. N. Evidence for Leaflet-Dependent Redistribution of Charged Molecules in Fluid Supported Phospholipid Bilayers. *Langmuir* **2008**, *24* (23), 13250−13253.
(39) Fang, Y.; Yang, J. The growth of bilayer defects and the induction of interdigitated domains in the lipid-loss process of supported phospholipid bilayers. *Biochim. Biophys. Acta, Biomembr.* **1997**, *1324* (2), 309−319.
(40) Anderson, T. H.; Min, Y.; Weirich, K. L.; Zeng, H.; Fygenson, D.; Israelachvili, J. N. Formation of Supported Bilayers on Silica Substrates. *Langmuir* **2009**, *25* (12), 6997−7005.
(41) Fadeel, B.; Xue, D. The ins and outs of phospholipid asymmetry in the plasma membrane: roles in health and disease. *Crit. Rev. Biochem. Mol. Biol.* **2009**, *44* (5), 264−277.
(42) Maret, W. Analyzing free zinc(ii) ion concentrations in cell biology with fluorescent chelating molecules. *Metallomics* **2015**, *7* (2), 202−211.
(43) Zago, M. P.; Verstraeten, S. V.; Oteiza, P. I. Zinc in the prevention of Fe2initiated lipid and protein oxidation. *Biol. Res.* **2000**, *33*, 143−150.
(44) Frederickson, C. J.; Suh, S. W.; Silva, D.; Frederickson, C. J.; Thompson, R. B. Importance of Zinc in the Central Nervous System: The Zinc-Containing Neuron. *J. Nutr.* **2000**, *130* (5), 1471S−1483S.
(45) Deutsch, J. W.; Kelly, R. B. Lipids of synaptic vesicles: relevance to the mechanism of membrane fusion. *Biochemistry* **1981**, *20* (2), 378−385.

https://dx.doi.org/10.1021/jacs.0c09103
J. Am. Chem. Soc. 2020, 142, 18679−18686